

Dynamic multidimensional optical networking based on spatial and spectral processing

Milorad Cvijetic,^{1,*} Ivan B. Djordjevic,¹ and Neda Cvijetic²

¹University of Arizona, Tucson, AZ 85721, USA
²NEC Laboratories America, Princeton, NJ 08540, USA
*milorad@optics.arizona.edu

Abstract: The recent introduction of optical OFDM and spatial MIMO techniques has led to considerable increases in spectral efficiency and aggregate throughput for future optical networks. However, these spatial and spectral domains can also be exploited for next-generation elastic optical networking. In this paper, we introduce the first hierarchy for dynamic multidimensional spatial and spectral optical networking and complement it with adaptive coded-modulation to form the basis of a novel elastic networking concept.

©2012 Optical Society of America

OCIS codes: (060.2330) Fiber optics communications; (060.4230) Multiplexing.

References and links

1. S. Gringeri, B. Basch, V. Shukla, R. Egorov, and T. J. Xia, "Flexible architectures for optical transport nodes and networks," *IEEE Commun. Mag.* **48**(7), 40–50 (2010).
2. M. Lee, J. Yu, Y. Kim, C. H. Kang, and J. Park, "Design of hierarchical crossconnect WDM networks employing two-stage multiplexing scheme at waveband and wavelength," *IEEE J. Sel. Areas Comm.* **20**(1), 166–171 (2002).
3. R. Izmailov, A. Kolarov, R. Fan, and S. Araki, "Hierarchical optical switching: a node-level analysis," *Proc. High Perf. Switching and Routing. Conf.*, 309–313 (2002).
4. W. Shieh and I. Djordjevic, *OFDM for Optical Communications* (Elsevier/Academic Press, 2009).
5. R. Schmogrow, M. Winter, M. Meyer, D. Hillerkuss, S. Wolf, B. Baeuerle, A. Ludwig, B. Nebendahl, S. Ben-Ezra, J. Meyer, M. Dreschmann, M. Huebner, J. Becker, C. Koos, W. Freude, and J. Leuthold, "Real-time Nyquist pulse generation beyond 100 Gbit/s and its relation to OFDM," *Opt. Express* **20**(1), 317–337 (2012).
6. T. Morioka, Y. Awaji, R. Ryf, P. Winzer, D. Richardson, and F. Poletti, "Enhancing optical communications with brand new fibers," *IEEE Commun. Mag.* **50**(2), s31–s42 (2012).
7. O. Gerstel, M. Jinno, A. Lord, and S. J. Ben Yao, "Elastic optical networking: a new dawn for the optical layer?" *IEEE Commun. Mag.* **50**(2), S12–S20 (2012).
8. B. Zhu, T. F. Taunay, M. F. Yan, J. M. Fini, M. Fishteyn, E. M. Monberg, and F. V. Dimarcello, "Seven-core multicore fiber transmissions for passive optical network," *Opt. Express* **18**(11), 11117–11122 (2010).
9. N. K. Fontaine, C. R. Doerr, M. A. Mestre, R. Ryf, P. Winzer, L. Buhl, Y. Sun, X. Jiang, and R. Lingle, "Space-division multiplexing and all-optical MIMO demultiplexing using a photonic integrated circuit," in *Optical Fiber Communication Conference*, OSA Technical Digest (Optical Society of America, 2012), paper PDP5B.1.
10. R. Ryf, R. Essiambre, A. Gnauck, S. Randel, M. A. Mestre, C. Schmidt, P. Winzer, R. Delbue, P. Pupalakis, A. Sureka, T. Hayashi, T. Taru, and T. Sasaki, "Space-division multiplexed transmission over 4200 km 3-core microstructured fiber," in *Optical Fiber Communication Conference*, OSA Technical Digest (Optical Society of America, 2012), paper PDP5C.2.
11. N. Bai, E. Ip, Y.-K. Huang, E. Mateo, F. Yaman, M.-J. Li, S. Bickham, S. Ten, J. Liñares, C. Montero, V. Moreno, X. Prieto, V. Tse, K. Man Chung, A. P. T. Lau, H.-Y. Tam, C. Lu, Y. Luo, G.-D. Peng, G. Li, and T. Wang, "Mode-division multiplexed transmission with inline few-mode fiber amplifier," *Opt. Express* **20**(3), 2668–2680 (2012).
12. T. Xia, G. A. Wellbrock, Y. Huang, M. Huang, E. Ip, P. N. Ji, D. Qian, A. Tanaka, Y. Shao, T. Wang, Y. Aono, and T. Tajima, "21.7 Tb/s field trial with 22 DP-8QAM/QPSK optical superchannels over 1,503-km of installed SSMF," in *Optical Fiber Communication Conference*, OSA Technical Digest (Optical Society of America, 2012), paper PDP5D.6.
13. I. B. Djordjevic, "Energy-efficient spatial-domain-based hybrid multidimensional coded-modulations enabling multi-Tb/s optical transport," *Opt. Express* **19**(17), 16708–16714 (2011).
14. Y. Zhang, M. Arabaci, and I. Djordjevic, "Rate-adaptive four-dimensional nonbinary LDPC-coded modulation for long-haul optical transport networks," in *Optical Fiber Communication Conference*, OSA Technical Digest (Optical Society of America, 2012), paper JW2A.46.
15. I. Djordjevic, T. Liu, L. Xu, and T. Wang, "Optimum signal constellation design for high-speed optical transmission," in *Optical Fiber Communication Conference*, OSA Technical Digest (Optical Society of America, 2012), paper OW3H.2.

1. Introduction

In current optical networks, the need to establish lightpaths (optical connection between two entities) in arbitrary directions, and switch them on-demand has led to the adoption of photonic routing devices mostly in the form of reconfigurable optical add-drop multiplexers (ROADM), and photonic crossconnects (PXC) [1]. With such technologies, optical switching and routing can be done at or above the per-wavelength level (i.e. “at the fiber level”). However, these optical switching and routing principles can only operate at per-wavelength or per-fiber granularity, which could increase complexity or reduce the bandwidth efficiency in future mixed-rate, heterogeneous optical networks with predominantly dynamic traffic demands. Switching at interim granularity – so-called waveband switching— has been also considered as an alternative [2,3]. The waveband concept has assumed that waveband consists of a number of wavelengths aligned to an ITU-T defined wavelength grid.

With the introduction of optical orthogonal frequency division multiplexing (OFDM) [4], or Nyquist-based pulse generation [5], novel frequency-domain degrees of freedom have been added to optical transmission. Moreover, with the advent of multicore and multimode optical fibers for throughput maximization [6], coarse switching at the fiber level may now require that the overall wavelength spectrum be switched not just from one fiber to another, *but from one spatial mode to another*. While previous work has considered physical-layer benefits of spatial mode (multimode and multicore) fiber transmission, to the best of our knowledge, no previous analysis exists on exploiting this spatial dimension for optical networking (i.e. switching and routing.) The spatial multiplexing domain (i.e. the use of multiple fiber core and/or spatial modes) thus emerges as a novel and appealing networking tool. Moreover, OFDM supercarriers (in all-optical Nyquist-based OFDM) and subcarriers (in electronic-based OFDM) emerge as *spectral* (i.e. frequency-domain) contributors to networking that can enable the spectral efficiency and granularity benefits needed for future elastic networks [7].

In this paper, we introduce and develop the first hierarchical structure for next generation dynamic optical networking based on novel multidimensional spatial and spectral processing. The roles of spatial multiple input multiple output (MIMO) techniques and OFDM supercarriers are defined and complemented by analysis of spectral/spatial interworking. Moreover, multidimensional elastic coded modulation is shown to be the third cornerstone of the overall agile optical networking scheme. By exploiting novel spatial/spectral domains in optical fiber, the proposed solution is promising for next-generation flexible optical networks.

2. Proposed multidimensional networking concept using spatial/spectral processing

The fundamental structure of a bandwidth granularity and multiplexing hierarchy at the entrance point of any specific optical fiber transmission line is shown in Fig. 1. As shown in Fig. 1, a number of independent lightpaths can be established through each fiber. In single mode fiber, two polarizations can be utilized to carry two independent signal streams. In multimode/multicore optical fibers, a number of independent spatial modes and polarizations can also be excited at the input of the fiber line. Furthermore, each independent lightpath can consist of multiple dense wavelength division multiplexed (DWDM) channels, each featuring a specific modulation and coding scheme. The spectral networking case with the highest flexibility and granularity is the scenario wherein Nyquist defined OFDM, both in the all-optical and electronic domains is adopted. Based on Fig. 1, several new dimensions for signal grooming, multiplexing and routing emerge as novel optical switching and routing tools and can be classified under two general categories:

1. *Spatial domain schemes:*

- Optical fibers as transmission entities (Level 6 from Fig. 1)
- Spatial MIMO arrangement (multiplexing) of lightpaths (Levels 3,4,5 from Fig. 1)

2. *Spectral (frequency) domain schemes:*

- Spectral arrangements within individual lightpaths featuring an ITU-T DWDM MUX structure, or supercarrier-based all-optical OFDM (Level 2 from Fig. 1)
- OFDM subcarrier arrangement within a specific carrier, with the modulation and signal processing performed at the electrical level (Level 1 from Fig. 1).

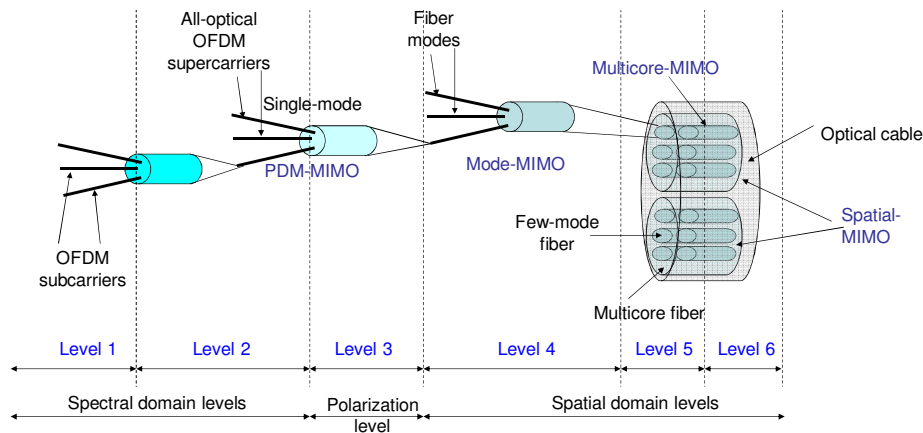


Fig. 1. Multidimensional (spatial + spectral) multiplexing hierarchy for dynamic optical networking.

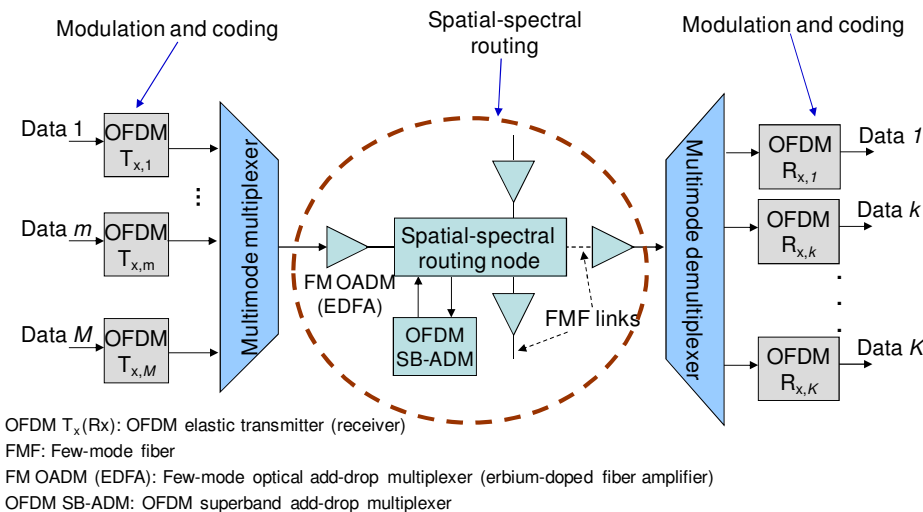


Fig. 2. Next-generation elastic optical network architecture with spatial and spectral processing.

The spatial MIMO approach has attracted a lot of attention recently in the fiber-optics research community, with a demonstration of all key elements needed for signal transmission, amplification and multiplexing/demultiplexing [8–11]. Transmission over 4200 km with 6 spatial modes has recently been reported [10]. Typically, the goal is to use MIMO as a means to increase the overall fiber transmission capacity by $M \times K$ -fold, where M and K are the number of independently transmitted and received signal modes, respectively. However, in the networking hierarchy proposed here, MIMO is viewed as a networking tool, in which multiple inputs are translated to multiple outputs of a $M \times K$ switching matrix, which, ideally, would be diagonal. From a physical-layer perspective, the MIMO switching matrix can thus arise from the use of either multicore or multimode fibers. There is significant networking potential in spatial domain multiplexing. For example, if we assume that mode launch and

detection can be accomplished by compact spatial multiplexers/demultiplexers [9], modes can be added/dropped dynamically, which is applicable for both multimode and multicore fibers.

The employment of the proposed spatial- spectral scheme in next-generation elastic optical networks is illustrated in Fig. 2. As shown in Fig. 2, the OFDM approach can be used in bandwidth elastic transponders at the optical transmission side in conjunction with both spectral and spatial multiplexing, all supported by the eventual adoption of novel optical fibers [6]. From Fig. 2, the key aspects of the proposed network include both a new spatial-spectral routing approach, as well as a multidimensional coded modulation scheme.

3. Spatial-spectral routing

The spatial-spectral routing node in Fig. 2 can maintain a generic hierarchical structure [2,3]. However, a significant difference emerges in the interpretation of both space and spectrum. Specifically, in this case, *space* represents a spatial mode rather than the physical fiber itself, and *spectrum* represents a number of adjacent all-optical OFDM supercarriers forming a “superband,” rather than a group of aggregated ITU-T wavelengths. To analyze the input/output allocation of the resulting approach, it is assumed that there is a total of M optical spatial inputs/outputs ($M = K$ case), and N optical spectral inputs (i.e. supercarriers). We wish to compute the spectral content per spatial input/output: the number of supercarriers, N_{avg} , assigned to a spatial output (i.e. the superband size). For simplicity, we assume the uniform case where all superbands are equal; this assumption can be further refined to a nonuniform case. It is also assumed that supercarriers within each superband would be pre-arranged by dynamic tuning and filtering. Finally, each supercarrier in a superband is assumed to have the same probability to be directed to any of the outgoing spatial modes.

The approach from [3] can then be invoked to analyze the superband size, N_{avg} , per spatial input/output, M . While in waveband routing schemes, such as the one in [3], considerable overlap and waste of up to 50% of individual spectral components may occur, in this case, since there is no fixed WDM grid, this number can be reduced, such that a lower fraction, ζ , of spectral components (supercarriers) would be wasted due to aggregation overlap during mapping to spatial outputs. The value $0 < \zeta \leq 0.25$ is selected here to halve the overhead permitted in the waveband routing scheme [3] and highlight the key difference between the legacy fixed WDM and proposed supercarrier-based approaches. The probability, ρ , that a specific supercarrier will be routed while carrying traffic then satisfies the relation $N \approx N\rho + \zeta$ (MN/I), where I denotes the number of superbands. Therefore, ρ can be expressed as $\rho \approx 1 - \zeta \times (M/I)$. Given that N supercarriers are randomly distributed to M spatial inputs, each spatial output gets N_{avg} supercarriers per superband with probability ρ , where N_{avg} is given by

$$N_{avg} = \sum_{n=1}^N n \binom{N}{n} \left(\frac{\rho}{M}\right)^n \left(1 - \frac{\rho}{M}\right)^{N-n}. \quad (1)$$

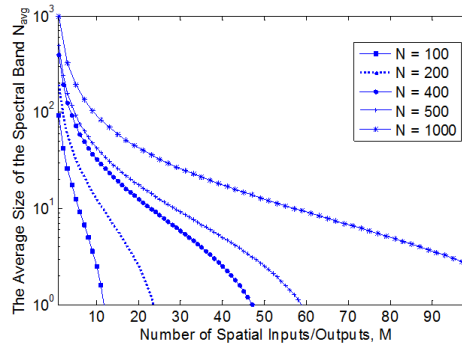


Fig. 3. Spectral superband size, N_{avg} , versus the number of spatial inputs/outputs, M .

Figure 3 plots the superband size, N_{avg} , versus the number of spatial inputs/outputs, M , for several values of total supercarriers, N and $\zeta = 0.25$. From Fig. 3, it can be seen that both high spectral throughputs and high networking flexibility can be achieved with a moderate number of spatial inputs/outputs. For example, with $N = 400$ total supercarriers and $I = 13$, $N_{avg} = 33$ supercarriers can be assigned to each of $M = 10$ spatial modes. Given that a 21.7Tb/s field trial using 330 optical OFDM supercarriers in a single mode was recently shown in [12], such target parameters are not far from current state-of-the-art. To date, up to 6 spatial modes per fiber have been experimentally multiplexed/demultiplexed [10], with on-going progress expected in the near future. Figure 3 also reveals high flexibility for M in the range reported in [8] and [10], via practical combinations for $N = 400$, such as $(M, N_{avg}) = (6, 60)$ and $(8, 43)$, for example. From Fig. 3, the combination $(M, N, N_{avg}) = (12, 400, 26)$ can be regarded as another practical indication of next steps to come. Relation (1) also reveals that for smaller values of M (e.g. $M < 12$), a decrease in ζ will not significantly alter the results of Fig. 3. As an example, for $\zeta = 0.12$, $(M, N, N_{avg}) = (11, 400, 33)$ will be obtained. However, for larger values of M , the corresponding family of curves for $\zeta = 0.12$ will drop-off more gradually.

4. Multidimensional coded-modulation for spectral/spatial networking

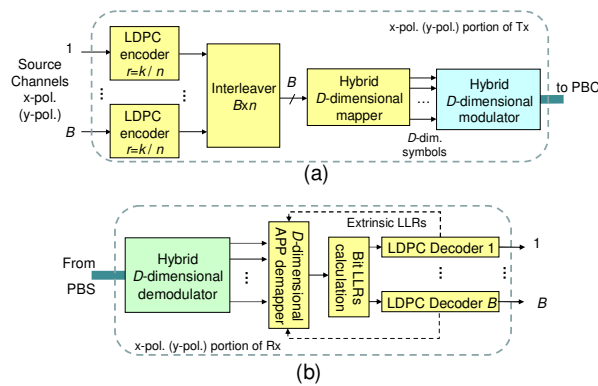


Fig. 4. Multidimensional hybrid LDPC-coded modulation scheme: (a) Tx and (b) Rx.

Multidimensional coded-modulation [13], seeks to employ the available degrees of freedom, namely: amplitude, phase, polarization, orthogonal subcarriers, and orbital angular momentum (OAM) in an elastic transmitter with dynamic bit rate adjustment. By increasing the number of dimensions, the aggregate data rate of the system can be increased dramatically while ensuring reliable transmission using capacity-approaching low density parity check (LDPC) codes. Apart from increasing the aggregate data rate, a D -dimensional space, when compared to the conventional two-dimensional (2D) space, can also increase the Euclidean distances between constellation points, and improve BER. The operational principle of multidimensional coded-modulation, which would be performed by the elastic transceiver arrays in Fig. 2, is depicted in Fig. 4. Since the elastic transceivers may also need to perform OAM crosstalk compensation and MIMO-based equalization to mitigate spatial coupling, the computational complexity would increase compared to 100Gb/s transponders. In each polarization, it is assumed that M_e electrical states, such as either orthogonal subcarriers or orthogonal polynomials, are employed. In addition, N_{OAM} orthogonal OAM states are used for modulation, such that the corresponding signal-space is $D = 2M_e N_{OAM}$ -dimensional. Independent binary streams are LDPC encoded, with corresponding codewords being written row-wise into a block-interleaver (see Fig. 4a). The B bits are taken column-wise from the block-interleaver and used to select the coordinates of the corresponding D -dimensional signal constellation. The output of the D -dimensional modulator (Fig. 4a) is then transmitted over the spatially multidimensional link. On receiver side (Fig. 4b), after D -dimensional demodulation, the outputs of the D branches of the demodulator are forwarded to the *a posteriori* probability (APP) demapper. The i -th branch in Fig. 4(b) represents the projection

along the i -th coordinate. The projections are used as inputs of the APP demapper, where symbol log likelihood ratios (LLRs) are calculated. Following the bit LLRs calculation block, the bit LLRs needed for LDPC decoding are calculated based on symbol LLRs. The extrinsic information is iterated between LDPC decoders and the APP demapper, until either valid codewords are obtained or the pre-determined number of iterations has been reached [14]. Instead of using conventional 2D constellations, we derive multidimensional ones by using: (i) centered iterative polar quantization (CIPQ), by placing one constellation point at the origin and determining the remaining constellation points by the IPQ approach [14]; and (ii) the optimum-signal constellation design (OSCD) algorithm [15].

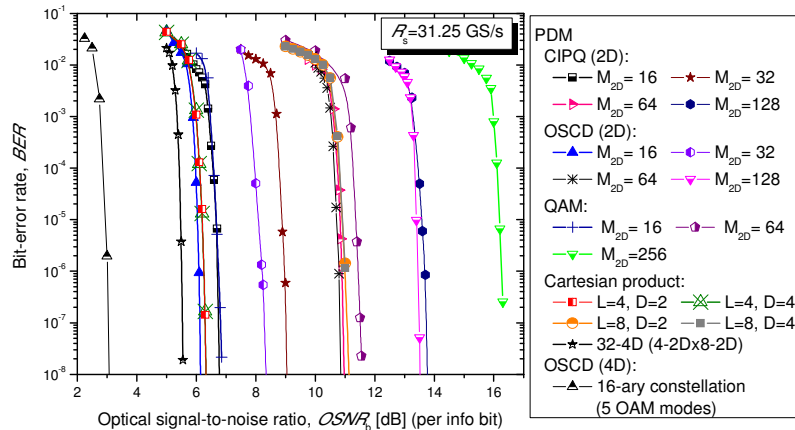


Fig. 5. BER performance of LDPC-coded multidimensional hybrid modulation versus conventional LDPC-coded PDM-QAM. M_{2D} : 2D signal constellation size.

Figure 5 plots the BER of the multidimensional hybrid LDPC-coded modulation scheme, for symbol rate $R_s = 31.25$ GS/s and large-girth LDPC code rate $r = 0.8$. The 2D signal constellations are obtained by maximizing the information rates, while larger dimensionality signal constellations are obtained as Cartesian products of optimized lower dimensionality constellations. As an illustration, 32-4D constellation is obtained as Cartesian product of 4-ary (QPSK) and optimum 8-ary 2D constellations. Figure 5 also plots corresponding conventional LDPC-coded PDM QAM curves as a reference case. From Fig. 5, it can be observed that at $BER = 10^{-7}$, the $L = 4$, $D = 4$ hybrid PDM coded modulation scheme outperforms corresponding PDM 256-QAM, which has the same number of constellation points, by almost 10 dB. Moreover, for a fixed number of amplitude levels per dimension (for signal constellations obtained as a Cartesian product of lower dimensionality ones) the increase in the number of dimensions results in negligible BER degradation as long as orthogonality of dimensions is preserved. By setting $L = 4$, $D = 7$, $R_s = 50$ GS/s, and $r = 0.8$, the aggregate data rate is 1.12 Tb/s/OAM mode, which is compatible with Tb/s Ethernet when one OAM mode is used. With four OAM modes, we achieve 4.48 Tb/s, which is compatible with future 4 Tb/s Ethernet. Figure 5 also plots BER for 16-ary 4D OSCD, which with five OAM modes and PDM achieves 1 Tb/s while significantly outperforming all other modulation schemes. We note that multidimensional coded-modulation both improves OSNR sensitivity and nonlinearity tolerance [14], enabling gains in transmission distance. Hybrid coded modulation can thus robustly and efficiently cover a broad range of bit rates for future elastic optical networks. Selection of the bit-rate and coded modulation scheme can also be dynamic, based on the overall transmission and networking constraints.

5. Conclusions

We have proposed the first hierarchical structure for next generation dynamic multidimensional optical networking based on novel spatial and spectral processing and coded

modulation. By exploiting novel spatial and spectral domains in optical fiber, the new scheme is a promising candidate for next-generation elastic optical networks.

Acknowledgments

This work was supported in part by the NSF under Grant CCF-0952711, NSF CIAN ERC under grant EEC-0812072, and NEC Laboratories America Inc.